THE ASTROPHYSICAL JOURNAL, 567:L115–L118, 2002 March 10


# *CHANDRA* OBSERVATIONS OF NGC 4636—AN ELLIPTICAL GALAXY IN TURMOIL

C. JONES, W. FORMAN, A. VIKHLININ, M. MARKEVITCH, L. DAVID, A. WARMFLASH, AND S. MURRAY
Harvard-Smithsonian Center for Astrophysics, 60 Garden Street, MS-31, Cambridge, MA 02138
AND
P. E. J. NULSEN
Department of Engineering Physics, University of Wollongong, Wollongong NSW 2522, Australia
*Received 2001 August 5; accepted 2002 February 7; published 2002 February 18*

## ABSTRACT

*Chandra* images show symmetric, 8 kpc long, armlike features in the X-ray halo surrounding NGC 4636. The leading edges of these features are sharp and are accompanied by temperature increases of ~30%. These properties suggest that the armlike structures are produced by shocks, driven by symmetric off-center outbursts. We interpret these observations as part of a cycle in which the cooling gas originally fueled a nuclear outburst about $3 \times 10^6$ yr ago that led to shocks reheating the cooling gas and thus preventing the accumulation of significant amounts of cooled gas in the galaxy center and temporarily starving the central active galactic nucleus.

*Subject headings:* galaxies: active — galaxies: individual (NGC 4636) — X-rays: galaxies

## 1. INTRODUCTION

NGC 4636 is one of the nearest and, at $L_X \sim 2 \times 10^{41}$ ergs $s^{-1}$, one of the most X-ray–luminous "normal" elliptical galaxies. NGC 4636 lies on the outskirts of the Virgo Cluster, 10° or 2.6 Mpc on the sky to the south of M87, for a distance to NGC 4636 of 15 Mpc (Tonry et al. 2001). As found for most luminous, slowly rotating elliptical galaxies, the optical surface brightness of NGC 4636 flattens in the inner regions. The central region, as seen in short exposures and with the *Hubble Space Telescope*, has low eccentricity and is classed as an E0. However, as noted by Sandage (1961), at low surface brightness, the galaxy is flattened (E4). NGC 4636 has ionized gas in its core but is unusual in that the gas velocities are uncorrelated with and significantly larger than those of the stars (Caon, Macchetto, & Pastoriza 2000). A weak, extended radio source ($1.4 \times 10^{38}$ ergs $s^{-1}$) is observed at the galaxy center (Birkinshaw & Davies 1985; Stanger & Warwick 1986), while Loewenstein et al. (2001) place an upper limit of $2.7 \times 10^{38}$ ergs $s^{-1}$ on nuclear X-ray emission.

*Einstein* X-ray images first showed that, like other luminous elliptical galaxies, NGC 4636 was surrounded by an extensive hot gas corona (Forman, Jones, & Tucker 1985). While *Einstein* observations allowed only an emission-weighted temperature to be determined, with *ROSAT* and *ASCA*, a modest increase in the gas temperature with radius was found, abundances in the halo were measured, and a very extended X-ray component was detected (Awaki et al. 1994; Trinchieri et al. 1994; Matsushita et al. 1997; Finoguenov & Jones 2000; Buote 2000). From an *Einstein* HRI observation, Stanger & Warwick (1986) found an asymmetric gas distribution that they suggested could be the result of erratic large-scale gas flows.

The *Chandra X-Ray Observatory* allows us to study the structure of the X-ray halo around NGC 4636 with a limiting resolution of ~50 pc. In this Letter, we present an analysis of the Advanced CCD Imaging Spectrometer (ACIS) observations that reveal unusual structures in the X-ray halo and describe a possible mechanism for producing these features.

## 2. *CHANDRA* X-RAY ANALYSIS

NGC 4636 was observed with ACIS-S for 53 ks on 2000 January 26–27 (observation 323) and with ACIS-I for 11 ks on 1999 December 4–5 (observation 324). We filtered the observations by selecting *ASCA* grades 0, 2, 3, 4, and 6 and eliminating intervals of high background ("flares") as well as bright columns or pixels due to instrumental effects or cosmic-ray afterglows. The remaining "good" times are 41,286 s in the ACIS-S observation and 5989 s in the ACIS-I observation.

Figure 1 shows the region of the ACIS-S3 CCD centered on NGC 4636 in the energy range from 0.5 to 2.0 keV. This image shows a bright central region surrounded by armlike structures. At a distance of 15 Mpc, these structures are observed to extend ~8 kpc from the galaxy center. While the features extending northeast (NE) and southwest (SW) are the brightest and appear symmetric around the galaxy center, the ACIS-S image shows a third, fainter arm northwest (NW) of the galaxy that shares symmetries with the two brighter X-ray arms. In particular, the sharp edges along the bright SW and faint NW arms define a parabola that also traces the southeast (SE) edge of the bright galaxy core. Part of this parabola is mirrored in the bright NE arm. There is additional structure especially in the eastern part of the halo.

To better define the halo structures, we generated a radial profile of the X-ray emission excluding the brighter regions noted above, as well as point sources, and used this profile to produce a smooth, radially symmetric, nonparametric two-dimensional model for the surface brightness. The right panel of Figure 1 shows the result of subtracting this model from the image in the left panel and smoothing the remaining emission. Most prominent in this figure are the enhanced regions of emission and the cavities to the east and west of the nucleus.

On larger scales, Figure 1 shows extended X-ray emission. This is likely the very extended emission found by *ROSAT* and *ASCA* (Trinchieri et al. 1994 and Matsushita et al. 1997). Although this extended emission was thought to be symmetric around NGC 4636, *Chandra* images show that it is brighter west of the galaxy. On small scales, Figure 2 shows that the X-ray emission in the galaxy core is elliptical (with a position angle of ~320°), with structure in the central 10″ region.

To study the bright armlike structures, we generated surface brightness distributions across the NE and SW arms and measured the gas temperature in several regions along and across these arms. As an example, the left panel of Figure 3 shows the X-ray surface brightness distribution projected along a rec-

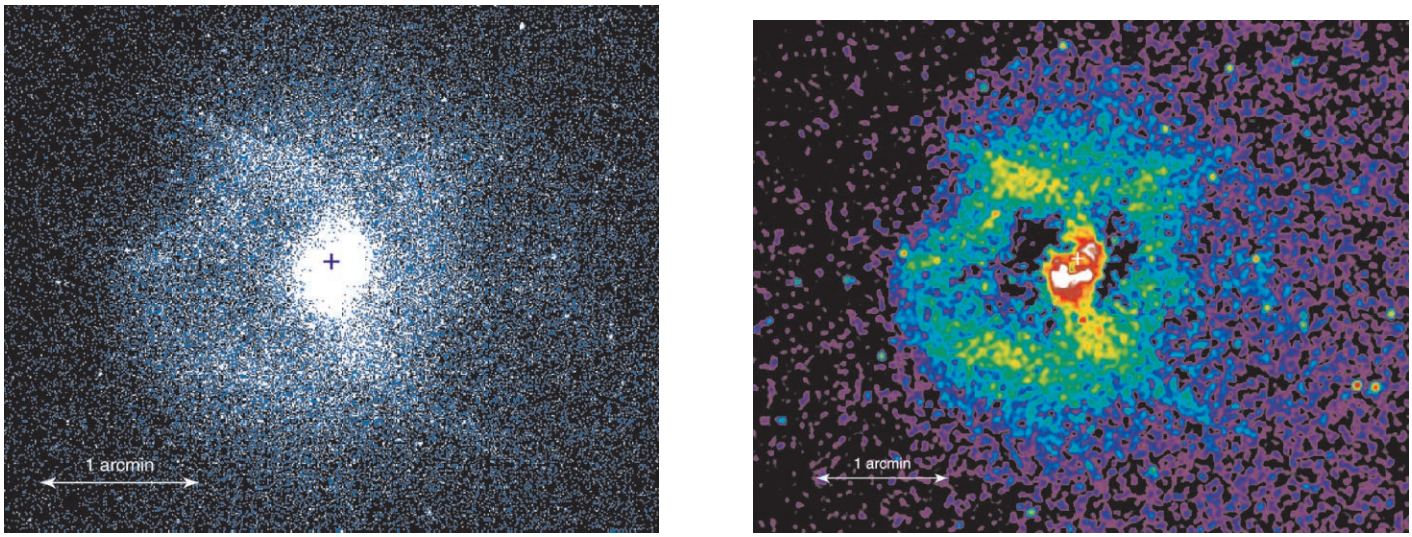


FIG. 1.—*Left*: ACIS-S image of NGC 4636 in the 0.5–2.0 keV energy range at full resolution (1 pixel = 0.″492). A plus sign marks the galaxy center. We suggest that shocks from a nuclear outburst produce the brighter armlike structures. *Right*: Emission after an azimuthally symmetric model describing the galaxy halo has been subtracted. The remaining emission was smoothed with a 2 pixel Gaussian. Features east of the central region could arise from another outburst.

tangle (55″ × 47″) centered 65″ from the nucleus and aligned parallel to the "leading" edge of the SW arm. As suggested in Figure 1, the projections show that the leading edges are remarkably sharp. Both arms show changes in brightness by about a factor of 2 on scales of a few arcseconds. The surface brightness falls more gradually toward the trailing edge.

To measure the gas temperature in these features, and throughout NGC 4636, we first identified and excluded regions around ~100 point sources in the ACIS-S3 CCD. To identify sources, we generated a 0.5–2.0 keV image without filtering for background flares. *Chandra*'s excellent angular resolution results in small "cells" for point sources, particularly near the telescope aim point. Thus, for point-source detection, the benefit of the longer exposure time gained by including times of high background outweighs the modest increase in the local background. We omitted point sources with at least nine counts. We also examined a "harder" 2.0–5.0 keV image to ensure that no highly absorbed sources were missed.

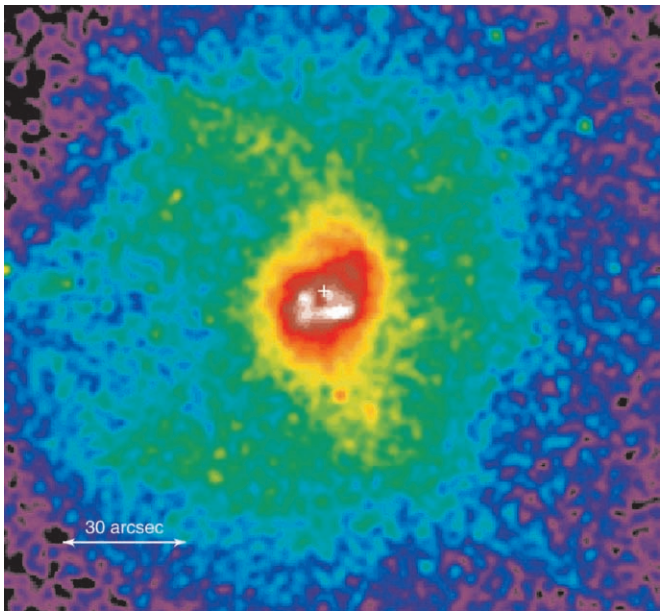


FIG. 2.—Central region in the 0.5–2 keV band smoothed with a 1.5 pixel Gaussian showing structure in the core and the intersection of the NE arm with the northern part of the core and the SW arm with the southern part of the core.

We extracted spectra for a variety of regions from the "cleaned image" and fitted these using MEKAL models in XSPEC with abundances from Anders & Grevesse (1989), over the energy range from 0.5 to 3 keV. Although the focus of this Letter is on the features in the hot halo, we first comment on the overall temperature structure. For several regions within the central bright core, we measured gas temperatures of 0.5 keV (with 90% uncertainties less than 0.03 keV) and abundances of 0.2 solar (assuming solar ratios for the heavy elements). Outside the central region, we observe a gradual rise in temperature from 0.5 to 0.7 keV within a radius of 3′ and a heavy-element abundance of 0.5–0.6 solar. This is consistent with the modest rise in temperature with radius reported by *ROSAT* (Trinchieri et al. 1994).

For the NE and SW arms, we measured the gas temperature both along and across these features. Along the arms, we found the same increase in gas temperature from 0.5 to 0.7 keV observed elsewhere in the halo. To reduce any biases that this radial temperature change could produce in looking for temperature changes across the arms, we extracted the spectra across each arm in two regions, centered 50″ and 80″ from the galaxy center. For each region, we extracted spectra in a series of rectangles (4″ × 27″) whose long sides were parallel to the sharp edge of each arm. For the arm regions closer to the galaxy center, where the halo emission is bright, we found no significant changes in the gas temperature across the arms. In particular, in the inner spectral regions of the NE arm, the best-fit temperatures range from 0.57 to 0.65 keV (with 90% uncertainties of 0.05 keV), while in the SW inner arm, the best-fit temperatures range from 0.60 to 0.68 keV. However, in the outer region of the SW arm, the spectra show significant changes in the gas temperature across the arm (see Fig. 3, *right*). For this region of the SW arm, if we take the temperature measurement south of the edge as the ambient temperature and fit the temperature in the arm with two components, one fixed at the temperature and normalization of the ambient region, the temperature of the second component is 1.0 ± 0.15 keV. In the NE arm, the temperature measured in

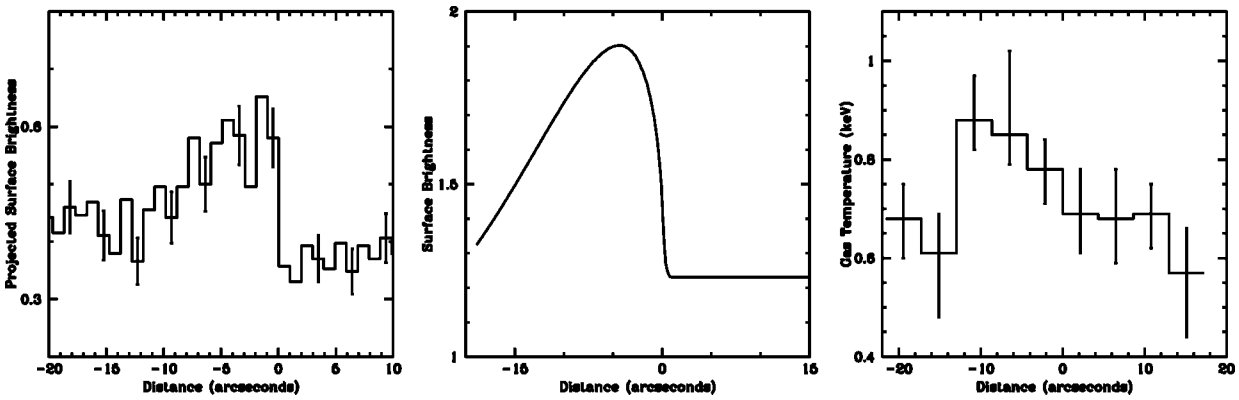


FIG. 3.—*Left*: Projected surface brightness across the SW arm. *Middle*: Expected surface brightness profile from the shock model. *Right*: Projected temperature profile across the SW arm. Error bars are 90% uncertainties. In each panel, the surface brightness discontinuity occurs at "0" on the *x*-axis.

the rectangle along the leading edge of the arm had the highest temperature ($0.77^{+0.07}_{-0.13}$ keV), but this was not significantly higher than in other regions. The smaller and less significant temperature changes in the NE arm may be due to contamination from emission from the other structures in the eastern part of the halo.

## 3. A NUCLEAR OUTBURST IN NGC 4636

While the X-ray features in NGC 4636 are so far unique, they share properties with structures seen in the hot gas in other galaxies and in clusters. The symmetric, parabolic regions of brighter emission resemble the X-ray bright filaments observed around the radio lobes in the elliptical galaxy M84 (Finoguenov & Jones 2000) and in the Hydra A and Perseus clusters (McNamara et al. 2000; Fabian et al. 2000). However, in NGC 4636, no large radio lobes are observed. In addition, while the sharpness of the edges of the NE and SW arms appears similar to the sharp edges found along "fronts" in clusters (Markevitch et al. 2000; Vikhlinin, Markevitch, & Murray 2001), the cluster fronts are cold, while those in NGC 4636 are hot.

While the presence of sharp fronts suggests the possibility of an ongoing merger, the east-west symmetry of the halo structures, the similarity of this structure to that seen around radio lobes, as well as the lack of a disturbed morphology in the stellar core or in the stellar velocities (Caon et al. 2000) led us to consider a nuclear outburst as the underlying cause. In particular, we interpret the bright SW arm, the fainter NW arm, and the bright NE arm as the projected edges of paraboloidal shock fronts expanding about an east-west axis through the nucleus, originating at two symmetric off-center locations. A shock model is also consistent with the evacuated cavities to the east and west of the central region (Fig. 1, *right*).

With this interpretation, we used the size as well as the surface brightness and temperature measurements of the SW arm to constrain a simple shock model. From our spectral measurements, the gas outside the arm has an ambient temperature $kT \sim 0.65$ keV. Taking the 1 keV temperature of the second spectral component in the SW arm as the postshock temperature, we can estimate the strength of the shock. A temperature jump by a factor of 1.75 arises from a shock having a density jump of a factor of 2 and a pressure jump of a factor of 3.5. The shock Mach number is 1.73, and the shock velocity is 725 km s$^{-1}$.

We computed the evolution of a shock front produced by a point explosion of $\sim 6 \times 10^{56}$ ergs in a uniform density gas. The state of this model is completely determined by the strength of the shock. We chose a time when the density jump is a factor of 2 for comparison with the observations. In our model, the surface brightness profile is determined by embedding the shocked region in a uniform cube of unshocked gas. The size of this cube relative to the size of the shocked region determines the amount of emission from unshocked gas and hence the size of the jump in surface brightness across the shock front. The center of the rectangle used to obtain the shock profile is ~65″ from the galaxy center. The length of the cube, $l$, is determined as the depth of gas, with the density of 0.012 cm$^{-3}$ measured at 65″ from the nucleus, that gives the observed surface brightness at this radius. Using $\beta$-model parameters for the undisturbed gas measured from the X-ray surface brightness profile ($\beta = 0.45$, core radius 8.″4) gives $l = 144''$ (10.4 kpc). At a radius of 65″, the diameter of the shocked region in NGC 4636 is $\simeq$107″, so the ratio of $l$ to the shock radius is ~2.7. With this value, we obtain the surface brightness distribution across the shock shown in Figure 3. We note that the shape of the shock front is not sensitive to the shock strength. The agreement between the surface brightness profiles derived from the observations and those derived from the model supports our interpretation of these features as shock fronts.

Our analysis assumes that the symmetry axis of the shocks lies in the plane of the sky. However, as shown in Figures 1 and 2, close to the center of the galaxy, the bright rim of the western parabola can be traced to the SE of the nucleus, while the edge of the eastern parabola can be traced to the NW of the nucleus. This overlap of the bases of the parabolas (the shock fronts) implies that the symmetry axis cannot be exactly in the plane of the sky. To determine the axis orientation, we would need the intrinsic shape of the shocked regions. This is constrained by the agreement between the observed and model shock profiles, and by the expectation that the shocked regions are not highly elongated. Both suggest that the symmetry axis is not far from the plane of the sky, but detailed modeling is needed to constrain this further.

Both the size and the symmetry of the apparent shocks point immediately to the nucleus as their energy source. Scaling from our simple model, the age of the shocks is $\sim 3 \times 10^6$ yr, and the total energy driving them is $\sim 6 \times 10^{56}$ ergs. This implies a modest mean nuclear output of $\sim 6 \times 10^{42}$ ergs s$^{-1}$. However, the absence of either strong X-ray or radio emission suggests that the active galactic nucleus (AGN) output is not constant over time. If the power of the outburst were near the Eddington limit for a $2 \times 10^8\ M_\odot$ black hole (Magorrian et al. 1998), then the required energy could be released in only ~1000 yr. This raises the possibility of very brief periods of quasar rebirth. We suggest that the other emission features in NGC 4636's

eastern halo originated from another nuclear outburst. The east-west asymmetry may result from projection effects, or they may result because the shocks have broken through to the east but so far have been confined by the denser medium west of the galaxy. Such outbursts could cause the large chaotic velocities found in the emission-line gas.

The narrow waist in the shocked region close to the nucleus suggests, in the simplest interpretation, that the energy driving the shocks was injected off-center, possibly via jets. Although the shape of the shocked regions favors off-center injection, the presence of only a weak, small-scale radio source in NGC 4636 argues against jets. Alternatively, since the speed of a strong shock is proportional to $\rho^{-1/2}$, if the unshocked gas is sufficiently dense close to the plane of the nucleus (perpendicular to the symmetry axis), then energy injected close to the nucleus can be channeled to produce shocks of this general shape. In fact, there is no real distinction between these; it is simply a matter of how far from the nucleus the energy is injected.

## 4. DISCUSSION

The hot gas in the centers of elliptical galaxies has a high density and thus a short cooling time. When the gas cools appreciably, it forms a dense disk because of rotation (Mathews & Brighenti 2000). If this cooled gas fuels a nuclear outburst that deposits energy close to the nucleus, the presence of the dense disk would channel the energy and produce shocks like those observed in NGC 4636. Thus, NGC 4636 appears to demonstrate the energy feedback process invoked to prevent the deposition of large quantities of cooled gas in the centers of galaxies and clusters (Tabor & Binney 1993; Churazov et al. 2001; David et al. 2001) as well as generate AGN cycles (e.g., Ciotti & Ostriker 1997). In a galaxy with the X-ray luminosity of NGC 4636, outbursts would need to occur every $\sim 5 \times 10^7$ yr to prevent the accumulation of a significant amount of cooled gas. If outbursts causing shocks occur every $5 \times 10^7$–$5 \times 10^8$ yr, then NGC 4636 and other elliptical galaxies could be in this shock phase 1%–10% of the time. If the outburst is fueled by cooled gas, then the repetition time must equal the central cooling time of the hot gas following an outburst. A typical elliptical galaxy, with a central cooling time of a few times $10^8$ yr, would be about halfway through this cycle. We recall that NGC 4636's X-ray luminosity is unusually high for its absolute magnitude compared with other early-type galaxies (Forman et al. 1985). This high X-ray luminosity may be due to the advanced state of cooling that brought on the outburst and may be further enhanced by the shocks. When the gas halo returns to hydrostatic equilibrium, its X-ray luminosity could decline by an order of magnitude or more, in which case the estimated outburst intervals would be much less frequent. Such excursions in X-ray luminosity would help explain the broad $L_X$-$L_B$ relation for elliptical galaxies.

Interactions between radio sources and the hot interstellar and intergalactic mediums in elliptical galaxies and clusters have been observed in a number of systems, e.g., Cen A (Kraft et al. 2000), M84 (Finoguenov & Jones 2000), Perseus (Böhringer et al. 1993), Hydra A (McNamara et al. 2000), and A2052 (Blanton et al. 2001). However, in these examples, the main observational characteristic is the displacement of hot gas by the radio-emitting lobes, while in approximate pressure equilibrium with the gas. In NGC 4636, we see evidence for a nuclear outburst, but no large radio lobes and only a relatively weak ($10^{38}$ ergs $s^{-1}$) central radio source. We suggest that the more common X-ray and radio lobe structures (e.g., M84) represent a later stage of the process seen in NGC 4636. This raises the issue of whether the nuclear outbursts that provide significant heating are primarily radio outbursts or whether radio outbursts occur in a phase following such an outburst. The latter scenario is consistent with the modest ratio of jet mechanical power to radio power found in Hydra A (McNamara et al. 2000).

In summary, the *Chandra* image shows new features in the X-ray halo of NGC 4636 that can be explained as the results of shocks produced by nuclear outbursts. We suggest that NGC 4636 is an example of the feedback process that prevents the deposition of significant amounts of cold gas by cooling flows. The lack of extended radio jets or lobes suggests that the energy from the AGN may be released by some more direct process rather than via a radio outburst.

We acknowledge stimulating discussions with E. Churazov and H. Donnelly. This work was supported by NASA contracts NAS8-38248 and NAS8-39073, the Chandra Science Center, and the Smithsonian Institution. P. E. J. N. gratefully acknowledges the hospitality of the Center for Astrophysics.

## REFERENCES

Anders, E., & Grevesse, N. 1989, Geochim. Cosmochim. Acta, 53, 197
Awaki, H., et al. 1994, PASJ, 46, L65
Birkinshaw, M., & Davies, R. 1985, ApJ, 291, 32
Blanton, E. L., Sarazin, C. L., McNamara, B. R., & Wise, M. W. 2001, ApJ, 558, L15
Böhringer, H., Voges, W., Fabian, A. C., Edge, A. C., & Neumann, D. M. 1993, MNRAS, 264, L25
Buote, D. 2000, ApJ, 539, 172
Caon, N., Macchetto, D., & Pastoriza, M. 2000, ApJS, 127, 39
Churazov, E., Bruggen, M., Kaiser, C., Böhringer, H., & Forman, W. 2001, ApJ, 554, 261
Ciotti, L., & Ostriker, J. P. 1997, ApJ, 487, L105
David, L. P., Nulsen, P. E. J., McNamara, B. R., Forman, W., Jones, C., Ponman, T., Robertson, B., & Wise, M. 2001, ApJ, 557, 546
Fabian, A. C., et al. 2000, MNRAS, 318, L65
Finoguenov, A., & Jones, C. 2000, ApJ, 539, 603
Forman, W., Jones, C., & Tucker, W. 1985, ApJ, 293, 102
Kraft, R. P., et al. 2000, ApJ, 531, L9
Loewenstein, M., Mushotzky, R. F., Angelini, L., Arnaud, K. A., & Quataert, E. 2001, ApJ, 555, L21
Magorrian, J., et al. 1998, AJ, 115, 2285
Markevitch, M., et al. 2000, ApJ, 541, 542
Mathews, W. G., & Brighenti, F. 2000, ApJ, 545, 181
Matsushita, L., Makishima, K., Rokutanda, E., Ymasaki, N., & Ohashi, T. 1997, ApJ, 488, L125
McNamara, B., et al. 2000, ApJ, 534, L135
Sandage, A. 1961, The Hubble Atlas of Galaxies (Washington, DC: CIW)
Stanger, V., & Warwick, R. 1986, MNRAS, 220, 363
Tabor, G., & Binney, J. 1993, MNRAS, 263, 323
Tonry, J., Dressler, A., Blakeslee, J., Ajhar, E., Fletcher, A., Luppino, G., Metzger, M., & Moore, C. 2001, ApJ, 546, 681
Trinchieri, G., Kim, D.-W., Fabbiano, G., & Canizares, C. 1994, ApJ, 428, 555
Vikhlinin, A., Markevitch, M., & Murray, S. 2001, ApJ, 551, 160